


 Cite this: *RSC Adv.*, 2025, **15**, 7973

Optimizing the white light emission in the solid state isatin and thiazole based molecular hybrids by introduction of variety of substituents on isatin and thiazole ring systems[†]

Sultana Shaik,^{‡,a} Rama Mohana Reddy Sirigireddy,^{‡,a} Sai Teja Talar,^{‡,a} Haranath Divi,^{‡,c} Naveen Mulakayala,^{‡,d} Venkatramu Vemula^{‡,b} and Chinna Gangi Reddy Nallagondu^{‡,a}

An efficient and practical 3-component reaction strategy has been developed for the synthesis of a series of multi-colour emissive isatin–thiazole based fluorophores, thiazolylhydrazoneindolin-2-ones (4) from readily available isatins (1), thiosemicarbazide (2) and α -bromoketones (3) in the presence of biodegradable citric acid (0.1 N) in ethanol at reflux temperature for 40–60 min. The reaction proceeds via condensation (C=N) and subsequent heterocyclization (C–S & C–N) in one-pot. Nature-friendly reaction profile, easy to perform, wide substrate scope, use of non-hazardous solvents/catalysts, good functional group tolerance, excellent yields (91–98%) in short reaction times, scalability and products do not require column chromatography purification are the attractive features of the present MCR strategy. The photophysical properties of the titled compounds (4) in both solid and solution states have been evaluated. The study reveals that the prepared isatin–thiazole based molecular hybrids exhibited tunable photophysical properties by varying the substituents on both isatin and thiazole motifs. To our delight, the titled compounds, 4k, 4l, 4m, 4u and 4y displayed white light emission with mega Stokes shifts in the solid state.

Received 25th December 2024
 Accepted 19th February 2025

DOI: 10.1039/d4ra09010a
rsc.li/rsc-advances

Introduction

Small organic luminophores emitting multicolour fluorescence in the solid state have a wide range of applications in full-color display panels and light sources.^{1–9} On the other hand, development of solid state light emissive fluorophores is really exigent assignment due to the aggregation-caused quenching (ACQ) in organic fluorophores. In this perspective, the intramolecular charge transfer (ICT) in organic luminophores is one of the challenging tasks for optoelectronic materials owing to the possibility for fine tuning of photophysical properties in the solid state.^{10–12} The photophysical properties of solid state

emissive organic fluorophores which includes absorption, emission, Stokes shifts, Commission Internationale d'Eclairage (CIE) coordinates and correlated colour temperature (CCT) have played a pivotal role in the fabrication of various optoelectronic devices like organic light-emitting diodes (OLEDs), organic solid state lasers and many others. Particularly, solid state white-light emitting small organic fluorophores (SWESOFs) received substantial societal attentions due to their unique merits like high efficiency, light-weight, longevity, high color quality, low-voltage operation, super-thin thickness, excellent compatibility, mercury-free device fabrication *etc.*, which signifying great affirm for solid state lighting (SSL) applications.^{13–21} Usually, white light emission is achieved mainly by integrating the stoichiometric ratios of primary colours of red, green and blue or blue and yellow. The CIE coordinates (x, y) for ideal white light is (0.33, 0.33), which is good for human eyesight. Hence, great efforts are devoted in both industry and academia for the development of solid state white light emitting small organic molecules with high fluorescence efficiency, low cost, low power consumption, high color purity, flexibility, ultra-thin thickness, stability, *etc.* Recently, we reported a few SWESOFs for optoelectronic applications.^{22,23} On the basis of our earlier studies on SWESOFs, herein, thiazole and isatin based small organic fluorophores

^aGreen & Sustainable Synthetic Organic Chemistry and Optoelectronics Laboratory, Department of Chemistry, Yogi Vemana University, Kadapa-516005, Andhra Pradesh, India. E-mail: ncgreddy@yogivemanauniversity.ac.in; ncgreddy@yvu.edu.in

^bDepartment of Physics, Yogi Vemana University, Kadapa-516 005, Andhra Pradesh, India. E-mail: vvrampuphd@gmail.com

^cDepartment of Physics, National Institute of Technology, Warangal-506004, Telangana, India

^dSVAK Lifesciences, ALEAP Industrial Area, Pragathi Nagar, Hyderabad 500090, India

[†] Electronic supplementary information (ESI) available: Spectral data, copies of ¹H-NMR & mass spectra, emission spectra, absorption spectra, CIE chromaticity diagram of isatin–thiazole based luminophores (4). See DOI: <https://doi.org/10.1039/d4ra09010a>

[‡] Equal contributors.



have been designed and developed for white light emission in the solid state.

Heterocycles containing nitrogen and sulphur atoms are amongst the most studied groups of small organic molecule emitters for example carbazoles, diazoles, triazoles, thiazoles, thiophenes *etc.*,²⁴ which have been utilized as efficient fluorescent organic materials for making optoelectronic devices, photovoltaics, *etc.*,^{25–28} because of their promising charge transfer and light-absorption properties. Further, two or more heterocyclic motifs containing small organic molecules are considered as another kind of compounds which display interesting optical properties.²⁹ In this context, thiazoles and isatins have received great attention due to their promising applications in both organic electronics and biological sciences. Thiazole compounds display promising optoelectronic and biological applications because these heterocyclic cores employed as fluorescent materials and key starting materials in the synthesis of lead molecules, new drug candidates, medicinally active compounds *etc.*^{22,23,30–35} In addition, this nucleus is found in several pharmaceutical drug molecules.^{36–39} Isatin group of compounds exhibit a wide spectrum of biological and optoelectronic properties.^{40–46} This core moiety has been found in many drugs like sunitinib, toceranib and nintedanib.^{47–49} Further, thiazole and isatin containing molecular hybrids also act as potent α -glucosidase inhibitors, anti-proliferative, anti-viral, anti-mycobacterial agents, *etc.*^{50–52} These molecular hybrids also act as hole transporting and ambipolar materials.⁵³ This motivated us to investigate the photophysical properties of thiazole and isatin based dyes. Up to now, a very limited protocols have been reported on both multi-component and multi-step reaction strategies for the synthesis of thiazolylhydrazoneindolin-2-ones from isatins, thiosemicarbazide and α -bromoketones.^{52,54–56} Though the reported methodologies are efficient for providing thiazolylhydrazoneindolin-2-ones, but suffer from some drawbacks such as limited substrate scope, long reaction times, use of expensive and toxic catalysts *etc.* In view of the above, identification of an efficient, practical, green and biodegradable catalytic system which fulfills the above limitations is highly desirable and challenging task for the synthesis of titled compounds.

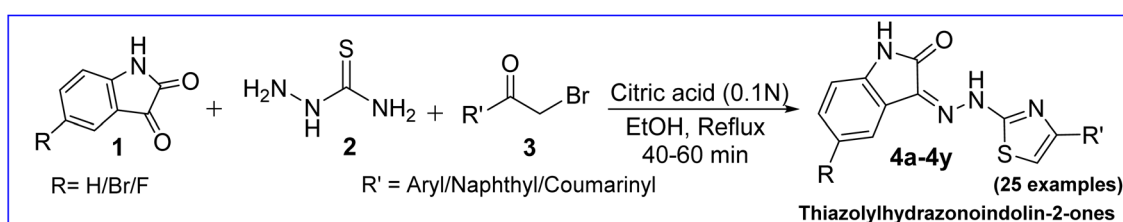
Citric acid is an organic acid which has great societal attentions because of its green merits which includes environmental-friendly nature, biodegradability, non-toxicity, excellent compatibility, inexpensiveness, *etc.* In spite of its nature-friendliness, a very few citric acid catalyzed organic

transformations have been reported so far.^{57–59} Hence, there is a wide scope to investigate the catalytic efficiency of citric acid in a variety of organic conversions.

Herein, citric acid (0.1 N) identified as environment friendly and biodegradable catalyst for the multi-component synthesis of thiazolylhydrazoneindolin-2-ones (**4**) *via* condensation and heterocyclization from readily available isatins (**1**), thiosemicarbazide (**2**) and α -bromoketones (**3**) in ethanol at reflux temperature in a single step operation (Scheme 1). Further, photophysical properties of the synthesized isatin-thiazole based fluorophores (**4**) have been investigated in both solid and solution states.

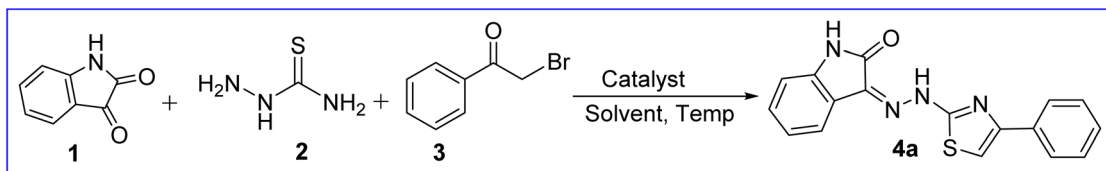
Results and discussion

Initially, a control experiment was performed to optimize the reaction conditions for the synthesis of thiazolylhydrazoneindolin-2-ones (**4**). For this purpose, isatin (**1a**), thiosemicarbazide (**2**) and ω -bromoacetophenone (**3a**) were chosen as ideal model substrates for the synthesis of 3-(2-(4-phenylthiazol-2-yl)hydrazinylidene)indolin-2-one (**4a**). At first, the model reaction was carried out in the absence of catalyst in H_2O at room temperature (Table 1, entry 1), it was found that the product has not been formed. Thereafter, the same reaction was repeated by screening various parameters like catalysts, solvents, temperature, and time to get the desired product (**4a**). Later, the same reaction was conducted in the presence of 0.1 N acetic acid in different solvents *i.e.*, acetone/isopropanol/ethanol (Table 1, entry 2). From this study, it was noticed that the reaction proceeded with a moderate yield (55%) of desired product (**4a**) in the presence of 0.1 N acetic acid (3.0 mL) in ethanol (3.0 mL) at reflux temperature in 90 min. Further, we aimed to develop the above 3-component reaction under green reaction conditions with environmental concerns in mind. To achieve the objective, various biodegradable α -hydroxy acid catalysts (malic acid, tartaric acid and citric acid) and different green solvents (acetone, isopropanol, and ethanol) were employed. The obtained results are summarized in Table 1. After the examination of various catalysts and solvents for the above-said reaction, it was found that the 3.0 mL of 0.1 N citric acid in EtOH (3.0 mL) was the most suitable catalytic medium to obtain high yield (80%) of the desired product (**4a**) at reflux temperature in 65 min (Table 1, entry 5). The other catalysts and solvents provided low to moderate yields of **4a** (Table 1, entries 3 and 4). Further, the amount of 0.1 N citric acid was varied (3.5, 4.0, 4.5, 5.0, 5.5, and



Scheme 1 Citric acid (0.1 N) catalyzed 3-component reaction for the synthesis of thiazolylhydrazoneindolin-2-ones (**4**).



Table 1 Optimization of reaction conditions for the synthesis of 3-(2-(4-phenylthiazol-2-yl)hydrazinylidene)indolin-2-one (4a)^a

Entry	Catalyst (3 mL)	Solvent (3 mL)	Temp. (°C)	Time (min)	Product	Yield ^b (%)
1 ^c	—	H ₂ O	RT	180	4a	—
2	Acetic acid (0.1 N)	Acetone	RT	90	4a	—
		Isopropanol	Reflux	90		45
		EtOH	Reflux	90		55
3	Malic acid (0.1 N)	Acetone	RT	90	4a	—
		Isopropanol	Reflux	90		25
		EtOH	Reflux	90		35
4	Tartaric acid (0.1 N)	Acetone	RT	90	4a	—
		Isopropanol	Reflux	90		45
		EtOH	Reflux	90		60
5	Citric acid (0.1 N)	Acetone	RT	90	4a	—
		Isopropanol	Reflux	90		55
		EtOH	Reflux	65		80

^a Reagents and conditions: isatin (1a) (5.0 mmol), thiosemicarbazide (2) (5.0 mmol), phenacyl bromide (3a) (5.0 mmol), catalyst (3 mL) & solvent (3 mL) at reflux/RT temperature. ^b Isolated yield. ^c Reaction performed in the absence of catalyst.

6.0 mL) to improve the yield of 4a (Table 2). The study reveals that the 5.0 mL of 0.1 N citric acid in EtOH (3.0 mL) at reflux temperature afforded the 97% yield of 4a within 45 min (Table 2, entry 5).

The yields of the product did not change when increasing the volume of 0.1 N citric acid (Table 2, entries 6 and 7). From this study, it was concluded that the said 3-component reaction proceeded smoothly in the presence of 0.1 N citric acid in EtOH and afforded the maximum yield of target product 4a.

Under the established reaction conditions in hand, the substrate scope with respect to substituted isatins (1a, 1b & 1c) and α -bromoketones (3a–j) was studied to investigate the generality of this MCR strategy. The obtained results are summarized in Table 3. The reaction of isatin (1a) thiosemicarbazide (2) and phenacyl bromide (3a) afforded the

corresponding product (4a) in excellent yield (97%). Similarly, phenacyl bromides substituted by activating groups (4-Me (3b), 4-OMe (3c)), deactivating groups (4-Cl (3e), 4-Br (3f), and 3-Br (3g)) and strongly deactivating groups (4-F (3d), 4-CN (3h)) provided the desired products (4b–h) in excellent yields (93–98%). Isatin (1a) reacted well with thiosemicarbazide (2) and 2-bromo-1-(naphthalen-2-yl)ethan-1-one (3i) also gave the corresponding product (4i) in good isolated yield (96%). Interestingly, isatin (1a) showed good reactivity with thiosemicarbazide (2) and 3-(2-bromoacetyl)-2H-chromen-2-one (3j) afforded the desired product (4j) in good isolated yield (95%).

Further, 5-bromo isatin (1b) was also reacted well with thiosemicarbazide (2) and various α -bromoketones (3a, 3b, 3d, 3g, 3i and 3j) and produced the corresponding products (4k–4p) in good to excellent yields (91–97%), respectively. 5-Fluoro isatin (1c) was also showed good reactivity with thiosemicarbazide (3) and variety of α -bromoketones (3a–3i) provided the desired products (4q–4y) in excellent yields ranging from 94–97%. Hence, the present MCR strategy well tolerates various substituents on the aromatic ring of α -bromoketones and isatins.

Table 2 Screening of catalyst loading in one-pot synthesis of 3-(2-(4-phenylthiazol-2-yl)hydrazinylidene)indolin-2-one (4a)^a

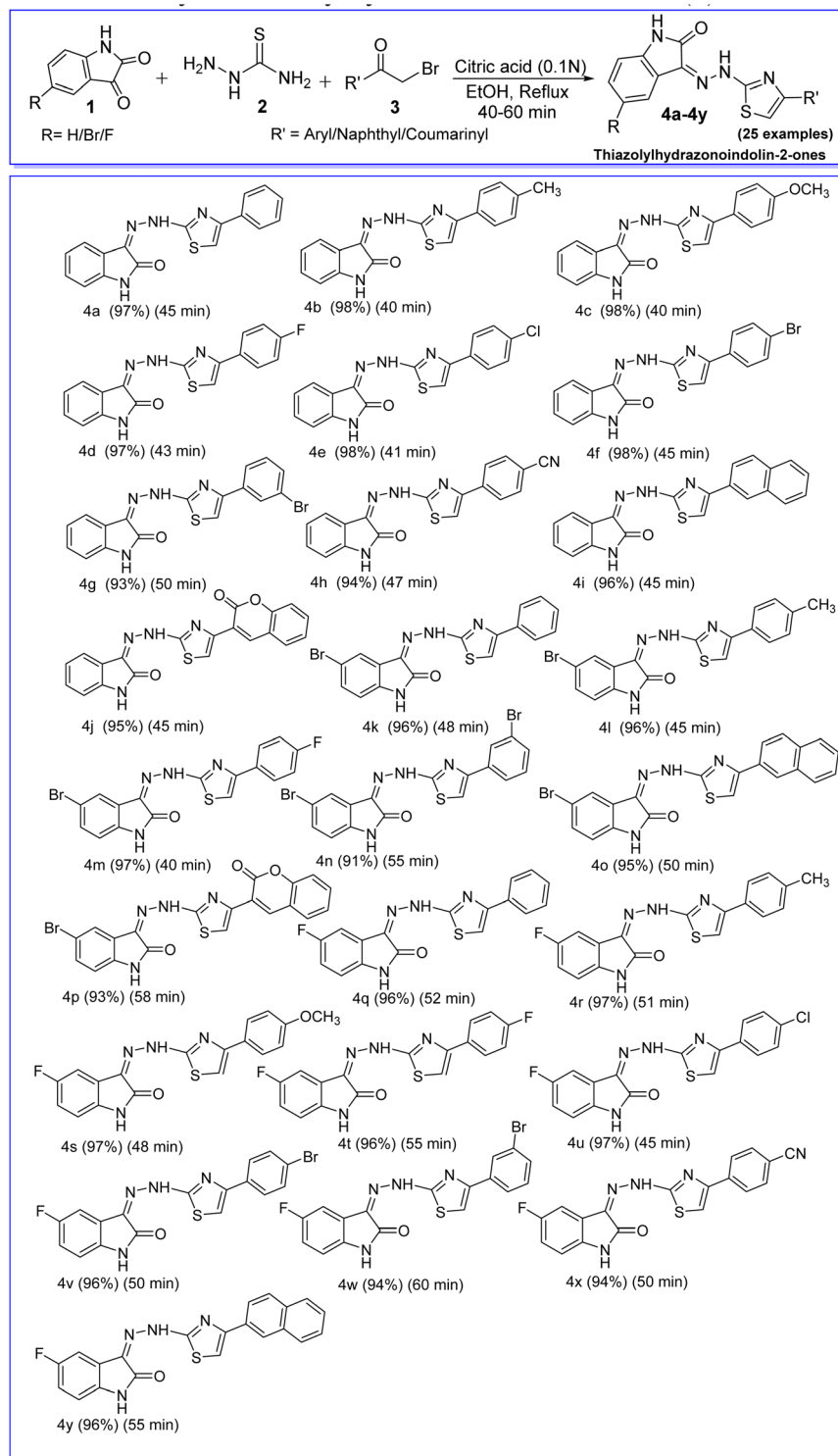
Entry	Citric acid (0.1 N) (mL)	Time (min)	Product	Yield ^b (%)
1	3.0	65	4a	80
2	3.5	60	4a	84
3	4.0	50	4a	89
4	4.5	45	4a	93
5	5.0	45	4a	97
6	5.5	45	4a	97
7	6.0	45	4a	97

^a Reagents and conditions: isatin (1a) (5.0 mmol), thiosemicarbazide (2) (5.0 mmol), phenacyl bromide (3a) (5.0 mmol), 0.1 N citric acid (mL), EtOH (3 mL) at reflux temperature. ^b Isolated yield.

Scalability

The scalability of the established procedure was then investigated by the reaction of isatin (1a), thiosemicarbazide (2) and 2,4'-dibromoacetophenone (3f) catalyzed by citric acid (0.1 N) in different gram-scale reactions (*i.e.*, 5.0, 10.0 and 15.0 g). The obtained yields of the product 4e were 98, 97, and 97%, respectively (Fig. 1). Hence, the developed 3-component reaction strategy is most suitable for the gram-scale production of thiazolylhydrazoneindolin-2-ones (4).



Table 3 Synthesis of a library of thiazolylhydrazoneindolin-2-ones (4)^a

Plausible mechanism

A plausible mechanism for the formation of thiazolylhydrazoneindolin-2-ones (4) in the presence of citric

acid (0.1 N) is depicted in Scheme 2. Firstly, the NH₂ group of thiosemicarbazide (2) reacts with citric acid (0.1 N) activated carbonyl group of isatins (1) to obtain thiosemicarbazone (I) via

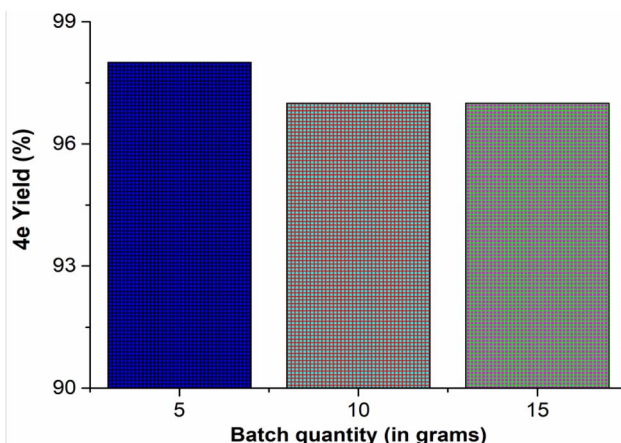


Fig. 1 Gram-scale synthesis of 4e.

a simple condensation reaction and then there is a loss of water by the condensation reaction of thiosemicarbazone (**I**) and α -bromo ketones (**3**) to form diimine (**II**). Further, the intermediate (**II**) undergoes internal S_N2 displacement of bromide ion in acid medium to form dihydrothiazolylhydrazoneindolin-2-ones (**III**) followed by a proton shift to obtain thiazolylhydrazoneindolin-2-ones (**4**). The high catalytic efficacy of citric acid in the present MCR might be due to the formation of 7-membered cyclic hydrogen bonding with both the carbonyl groups of isatins and α -bromo ketones.⁶⁰

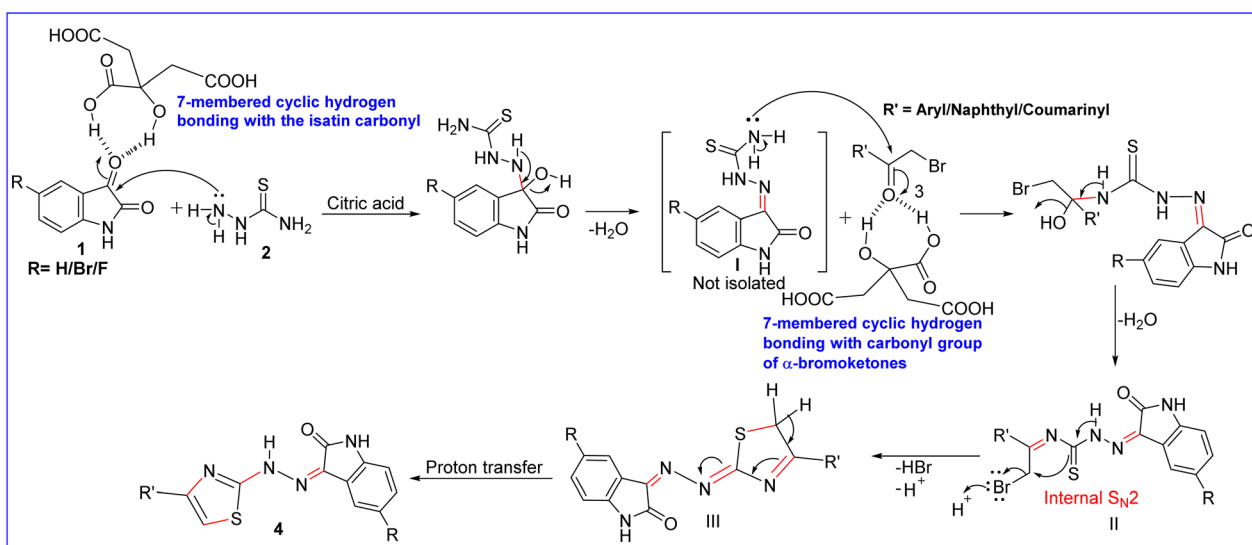
Photophysical properties of thiazolylhydrazoneindolin-2-ones (**4**)

The photophysical properties of a library of synthesized titled compounds (**4**) were studied in both solid and solution states from their absorption spectra and luminescence spectra and are shown in Table 4. The solubility of the synthesized thiazolylhydrazoneindolin-2-ones (**4**) was examined in various

polar solvents like isopropanol, acetone, acetonitrile, dichloromethane, ethyl acetate, dimethylformamide (DMF) and dimethyl sulfoxide (DMSO). The study reveals that the titled compounds (**4**) are freely soluble in polar aprotic DMSO at RT as compared to other solvents. Therefore, the photophysical properties of **4** in the solution state were investigated in DMSO. The Stokes shifts, CIE coordinates, CCT values and quantum yields were determined and discussed hereunder.

Organic fluorescent molecules with large (mega) Stokes shifts (≥ 80 nm) can avoid the cross-relaxation results in efficient emission spectra. This indicates that there is no self-quenching by reabsorption and it makes possible to record the fluorescence spectra even with low cost spectrometer. Further, the organic fluorescent material with mega Stokes shift is the desired characteristic property to eliminate self-absorption or the inner filter effect. Hence, the development of fluorophores with mega Stokes shifts and high brightness is highly essential for optoelectronic applications.^{61,62}

The Stokes shifts of thiazolylhydrazoneindolin-2-ones (**4**) have been calculated from the emission and absorption spectra (Fig. 2a-j, 3a-j, S68, S69, S70 and S71†). The results obtained are presented in Table 4. The study reveals that the Stokes shifts are influenced by the substituents on isatin and thiazole rings of the titled compounds (**4**). Interestingly, all the titled compounds displayed a very large Stokes shifts in the solid state when compared to the solution state. Initially, Stokes shifts of compounds, **4a-4j** are influenced by only the substituents at 4th position of thiazole ring. For instance, the electron donating *p*-methoxyphenyl (*p*-OMePh) and *p*-methylphenyl (*p*-MePh) groups at the 4th position of thiazole ring of **4c** and **4b** were bathochromically shifted with a large Stokes shift as compared to the electron withdrawing *p*-cyanophenyl (*p*-CNPh) group at the same position of thiazole ring of **4h** in both solid and solution states (Table 4, entries 2, 3 and 8). The *p*-bromophenyl (*p*-BrPh) group at the 4th position of thiazole ring of **4f** was red shifted with a large Stokes shift as compared to the *p*-

Scheme 2 A plausible mechanism for the formation of thiazolylhydrazoneindolin-2-ones (**4**) in the presence of citric acid (0.1 N).

fluorophenyl (*p*-FPh), *p*-chlorophenyl (*p*-ClPh) and *m*-bromophenyl (*m*-BrPh) groups at the 4th position of thiazole ring of **4d**, **4e** and **4g**, respectively in the solid-state whereas, **4e** was red shifted with a large Stokes shift as compared to **4d**, **4f** and **4g** in the solution state (Table 4, entries 4–7).

The phenyl (Ph) group at 4th position of thiazole ring of **4a** and β -naphthyl group at 4th position of thiazole ring of **4i** were bathochromically shifted with a large Stokes shift as compared to coumarinyl group at the same position of thiazole ring of **4j** in the solid-state but, **4a** in solution state was blue shifted than **4i** and **4j** (Table 4, entries 1, 9 and 10). Next, the effect of bromo substituent at 5th position of the isatin and various substituents at 4th position of thiazole rings on Stokes shifts was studied. For example, electron donating *p*-methylphenyl (*p*-MePh) at 4th position of thiazole ring of **4l** in the solid-state was red shifted with a large Stokes shift and the same was red shifted with a small Stokes shift in solution state when compared to the *p*-fluorophenyl (*p*-FPh) and *m*-bromophenyl (*m*-BrPh) groups at the 4th position of thiazole ring of **4m** and **4n**, respectively (Table 4, entries 12–14). Interestingly, compound **4n** showed a small Stokes shift as compared with other derivatives in both solid and solution states. This might be due to the presence of bromo substituent on both isatin and phenyl ring of thiazole. The phenyl (Ph) group at 4th position of thiazole ring of **4k** was blue shifted with a large Stokes shift and was also

bathochromically shifted with a mega Stokes shift as compared to the β -naphthyl and coumarinyl group at the same position of thiazole ring of **4o** and **4p**, respectively in the solid-state whereas **4k** was blue shifted as compared to **4o** and **4p** with a small and large Stokes shifts, respectively (Table 4, entries 11, 15 and 16). Further, the effect of fluoro substituent at 5th position of the isatin and a variety of substituents at 4th position of thiazole rings on Stokes shifts was also investigated. For instance, the electron donating *p*-methylphenyl (*p*-MePh) and *p*-methoxyphenyl (*p*-OMePh) groups at 4th position of thiazole ring of **4r** and **4s** were bathochromically shifted with a large Stokes shift as compared to the electron withdrawing *p*-cyanophenyl (*p*-CNPh) group at the same position of thiazole ring of **4x** in the solid-state but **4r** was blue shifted with a small Stokes shift and **4s** was red shifted with a large Stokes shift than **4x**, respectively in the solution state (Table 4, entries 18, 19 and 24). The *m*-bromophenyl (*m*-BrPh) group at the 4th position of thiazole ring of **4w** was slightly red shifted with a mega Stokes shift as compared to the *p*-fluorophenyl (*p*-FPh) and *p*-chlorophenyl (*p*-ClPh) groups at the 4th position of thiazole ring of **4t** & **4u** and was slightly blue shifted with a mega Stokes shift when compared to the *p*-bromophenyl (*p*-BrPh) group at the same position of thiazole ring of **4v** in the solid-state. Whereas in the solution state, **4t** was red shifted with a large Stokes shift as compared to **4w** and was slightly blue-shifted with a large Stokes

Table 4 Photophysical properties of thiazolylhydrazoneindolin-2-ones (4)

Entry	Comp.	λ_{exi}^a (nm)		λ_{abs}^b (nm)		λ_{emi}^c (nm)		Stokes shift ^d (cm ⁻¹ nm ⁻¹)		CIE coordinates				CCT ^e (K)
		Solid	DMSO	Solid	DMSO	Solid	DMSO	Solid	DMSO	x	y	x	y	
1	4a	368	352	553	432	9091/185	5261/80	0.41	0.57	0.19	0.21	—	—	
2	4b	368	350	578	430	9873/210	5315/80	0.50	0.44	0.20	0.24	—	—	
3	4c	370	369	580	534	9786/210	8373/165	0.51	0.44	0.26	0.54	—	—	
4	4d	368	354	558	430	9253/190	4993/76	0.43	0.55	0.19	0.21	—	—	
5	4e	368	352	559	433	9285/191	5314/81	0.43	0.55	0.17	0.16	—	—	
6	4f	368	352	565	430	9475/197	5153/78	0.47	0.52	0.20	0.23	—	—	
7	4g	370	352	542	428	8577/172	5044/76	0.36	0.60	0.18	0.18	—	—	
8	4h	368	357	559	436	9285/191	5075/79	0.43	0.55	0.17	0.15	—	—	
9	4i	370	362	557	451	9074/187	5451/89	0.41	0.50	0.18	0.21	—	—	
10	4j	371	361	536	448	8297/165	5379/87	0.34	0.62	0.16	0.15	—	—	
11	4k	348	346	586	420	11 671/238	5092/74	0.48	0.40	0.16	0.10	2225	—	
12	4l	370	362	584	435	9904/214	4636/73	0.41	0.34	0.17	0.12	2913	—	
13	4m	370	359	569	433	9452/199	4760/74	0.41	0.41	0.17	0.12	3554	—	
14	4n	503	352	565	392	2182/62	2899/40	0.42	0.49	0.15	0.08	—	—	
15	4o	372	397	589	518	9904/217	5884/121	0.50	0.41	0.23	0.62	—	—	
16	4p	370	362	550	438	8845/180	4793/76	0.38	0.59	0.23	0.62	—	—	
17	4q	370	362	582	440	9845/212	4897/78	0.5	0.47	0.16	0.13	—	—	
18	4r	368	361	576	437	9813/208	4817/76	0.49	0.45	0.17	0.14	—	—	
19	4s	370	362	581	441	9815/211	4948/79	0.47	0.44	0.16	0.14	—	—	
20	4t	368	354	574	434	9752/206	5207/80	0.45	0.47	0.18	0.15	—	—	
21	4u	367	360	572	436	9765/205	4842/76	0.44	0.41	0.16	0.12	3001	—	
22	4v	368	360	580	436	9933/212	4842/76	0.46	0.46	0.17	0.12	—	—	
23	4w	338	342	578	414	12 285/240	5085/72	0.49	0.50	0.16	0.11	—	—	
24	4x	368	362	560	440	9317/192	4897/78	0.35	0.48	0.16	0.12	—	—	
25	4y	370	362	593	438	10 164/223	4793/76	0.46	0.36	0.19	0.17	2232	—	

^a Excitation measured in the solid state. ^b Absorption measured in the solution state. ^c Emission measured in both solid and solution states.

^d Stokes shift; $\Delta\nu = \nu_{\text{abs},\text{max}} - \nu_{\text{emis},\text{max}}$; $\Delta\lambda = \lambda_{\text{emis},\text{max}} - \lambda_{\text{abs},\text{max}}$. ^e CCT = $-449n^3 + 3525n^2 - 6823n + 5520.33$; here $n = (x - x_c)/(y - y_c)$, $x_c = 0.3320$ and $y_c = 0.1858$.



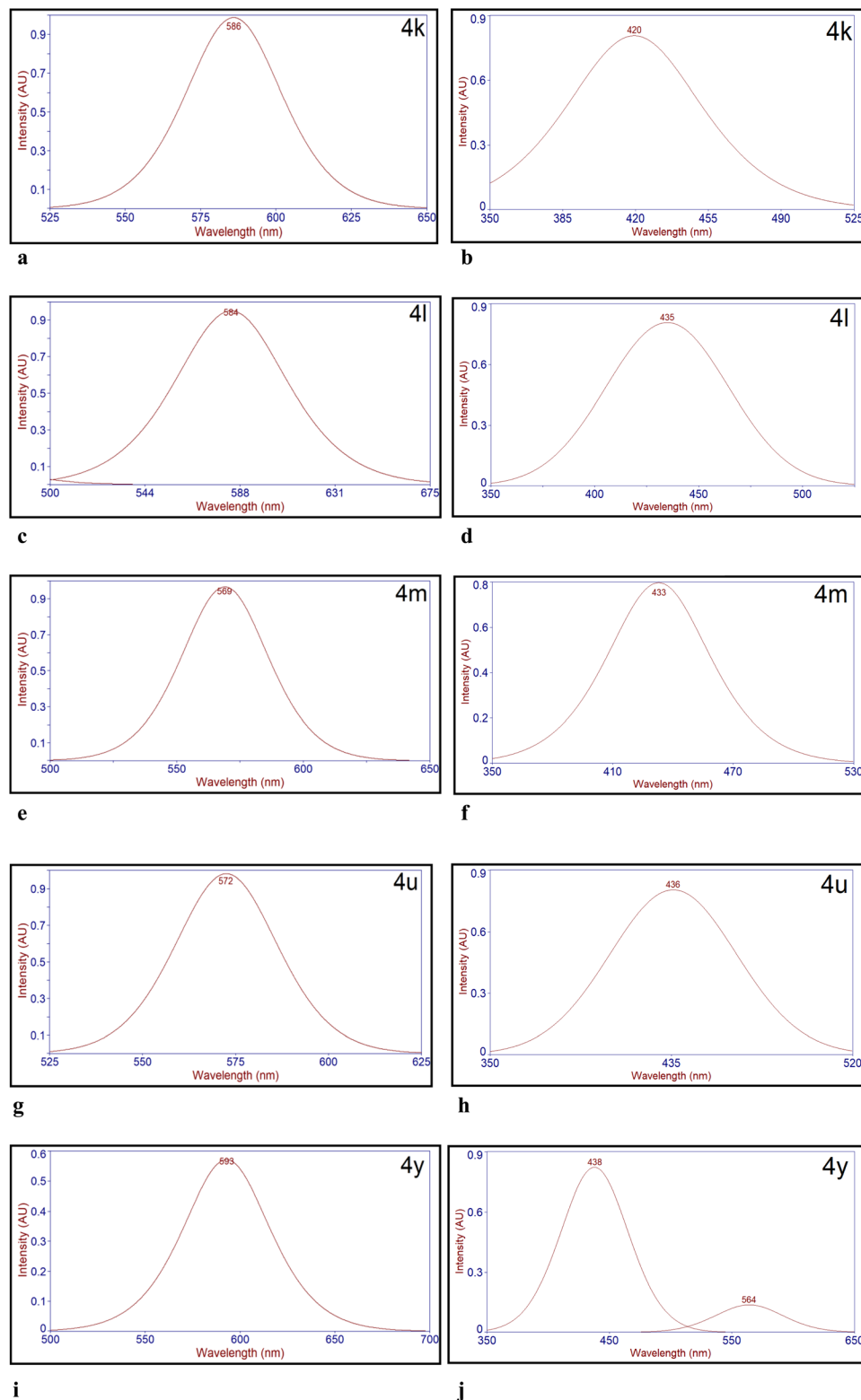


Fig. 2 (a) Deconvoluted solid state emission spectrum of **4k**. (b) Deconvoluted emission spectrum of **4k** in DMSO (1.0×10^{-5} M). (c) Deconvoluted solid state emission spectrum of **4l**. (d) Deconvoluted emission spectrum of **4l** in DMSO (1.0×10^{-5} M). (e) Deconvoluted solid state emission spectrum of **4m**. (f) Deconvoluted emission spectrum of **4m** in DMSO (1.0×10^{-5} M). (g) Deconvoluted solid state emission spectrum of **4u**. (h) Deconvoluted emission spectrum of **4u** in DMSO (1.0×10^{-5} M). (i) Deconvoluted solid state emission spectrum of **4y**. (j) Deconvoluted emission spectrum of **4y** in DMSO (1.0×10^{-5} M).



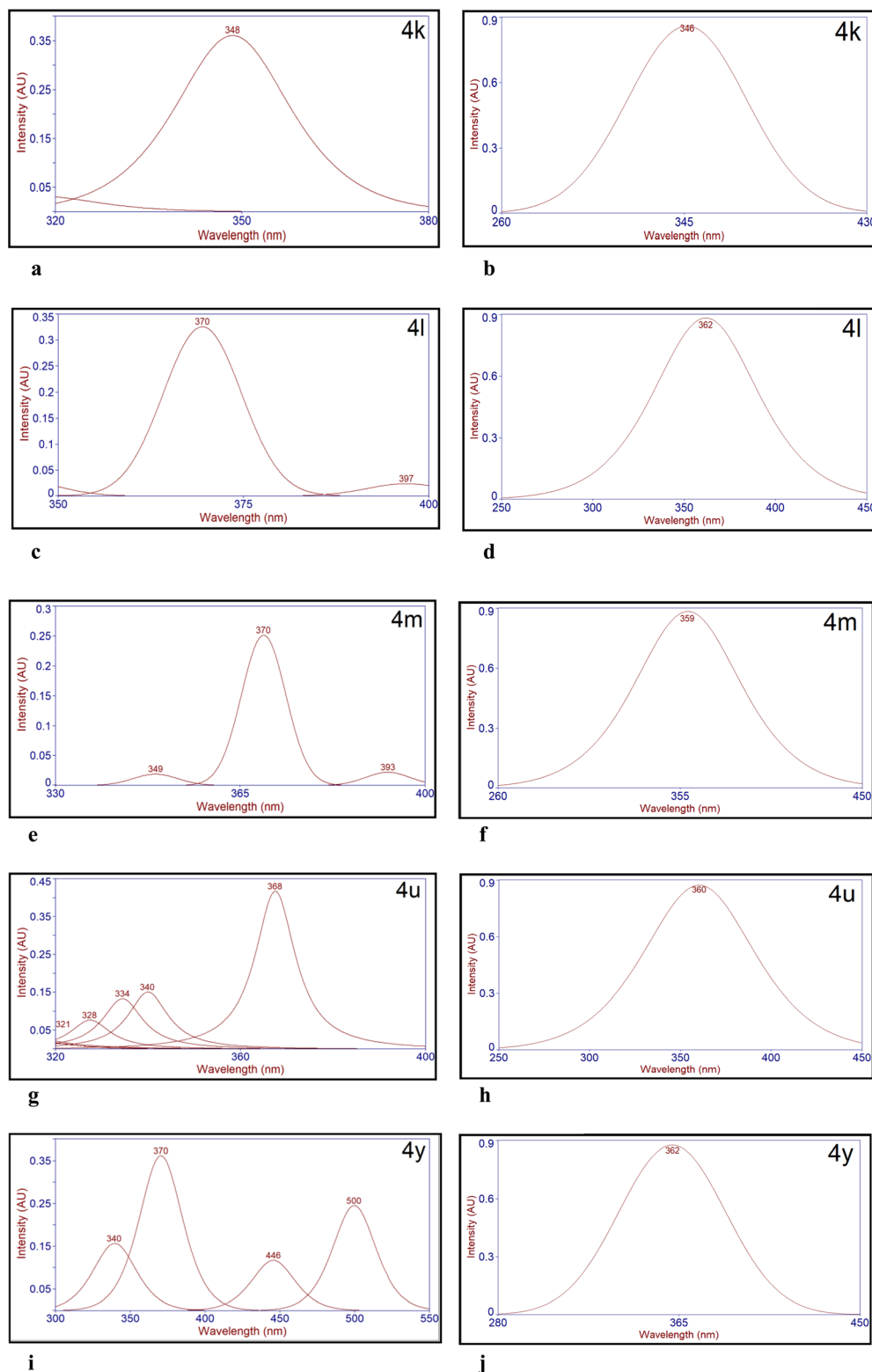


Fig. 3 (a) Deconvoluted solid state excitation spectrum of **4k**. (b) Deconvoluted absorption spectrum of **4k** in DMSO (1.0×10^{-5} M). (c) Deconvoluted solid state excitation spectrum of **4l**. (d) Deconvoluted absorption spectrum of **4l** in DMSO (1.0×10^{-5} M). (e) Deconvoluted solid state excitation spectrum of **4m**. (f) Deconvoluted absorption spectrum of **4m** in DMSO (1.0×10^{-5} M). (g) Deconvoluted solid state excitation spectrum of **4u**. (h) Deconvoluted absorption spectrum of **4u** in DMSO (1.0×10^{-5} M). (i) Deconvoluted solid state excitation spectrum of **4y**. (j) Deconvoluted absorption spectrum of **4y** in DMSO (1.0×10^{-5} M).

shift than **4u** and **4v**, respectively (Table 4, entries 20–23). The β -naphthyl group at 4th position of thiazole ring of **4y** was bathochromically shifted with a large Stokes shift as compared to the phenyl (Ph) group at the same position of thiazole ring of **4q** in the solid state but **4y** was blue shifted with a small Stokes shift as compared to **4q** in the solution state (Table 4, entries 17 and 25). To our delight, the compounds, **4k**, **4l**, **4m**, **4u** and **4y** in the solid state exhibited mega Stokes shifts $11\,671\text{ cm}^{-1}$ (238 nm), 9904 cm^{-1} (214 nm), 9452 cm^{-1} (199 nm), 9765 cm^{-1} (205 nm) and $10\,164\text{ cm}^{-1}$ (223 nm), respectively. From this study, it was clearly stated that there is no self-quenching by reabsorption.

Optimization of white light emission: CIE colour coordinates and CCT values

To optimize the white light emission in the isatin–thiazole based fluorophores (**4**), a variety of groups/substituents have been introduced on 4th position of thiazole and 5th position of isatin ring systems.

The CIE colour coordinates (x , y) of thiazolylhydrazoneindolin-2-ones (**4**) have been evaluated from the emission spectra (Fig. 2a–j, S68 and S70†) at different excitation wavelengths by adopting the reported procedure.⁶³ The obtained results are summarized in Table 4. The colour coordinates of multi-colour emissive fluorophores (**4**) are shown in Fig. 4a, b and S72,† From CIE colour coordinates (x , y), it was observed that the colour tunability of **4** mainly depends on both the substituents present on isatin and the substituents at the 4th position of thiazole ring of **4**. At first, CIE colour coordinates have been calculated for the compounds, **4a**–**4j** which were prepared from simple isatin (**1a**), thiosemicarbazide (**2**) and various α -bromoketones (**3a**–**3j**). From this study, it was found that the **4a** (Ph), **4d** (*p*-FPh), **4e** (*p*-ClPh) and **4h** (*p*-CNPh) emitted yellowish green light emission excited at 368 nm in the solid state (Table 4, entries 1, 4, 5 and 8). The compounds, **4b** (*p*-MePh; $\lambda_{\text{exi}} = 368\text{ nm}$) and **4c** (*p*-OMePh; $\lambda_{\text{exi}} = 370\text{ nm}$) showed yellowish orange light emission (Table 4, entries 2 and 3). The fluorophores, **4f** (*p*-BrPh; $\lambda_{\text{exi}} = 368\text{ nm}$) and **4i** (β -naphthyl; $\lambda_{\text{exi}} = 370\text{ nm}$) exhibited greenish yellow light emission (Table 4, entries 6 and 9). The compounds, **4g** (*m*-BrPh; $\lambda_{\text{exi}} = 370\text{ nm}$) and **4j** (coumarinyl; $\lambda_{\text{exi}} = 371\text{ nm}$) displayed yellowish green light emission (Table 4, entries 7 and 10). Whereas in the solution state, **4a** (Ph; $\lambda_{\text{exi}} = 352\text{ nm}$), **4d** (*p*-FPh; $\lambda_{\text{exi}} = 354\text{ nm}$), **4e** (*p*-ClPh; $\lambda_{\text{exi}} = 352\text{ nm}$), **4g** (*m*-BrPh; $\lambda_{\text{exi}} = 352\text{ nm}$), **4h** (*p*-CNPh; $\lambda_{\text{exi}} = 357\text{ nm}$), **4i** (β -naphthyl; $\lambda_{\text{exi}} = 362\text{ nm}$) and **4j** (coumarinyl; $\lambda_{\text{exi}} = 361\text{ nm}$) exhibited blue light emission (Table 4, entries 1, 4, 5, 7–10). The compounds, **4b** (*p*-MePh; $\lambda_{\text{exi}} = 350\text{ nm}$) and **4f** (*p*-BrPh; $\lambda_{\text{exi}} = 352\text{ nm}$) showed greenish blue light emission in the solution state (Table 4, entries 2 and 6). The compound **4c** (*p*-OMePh; $\lambda_{\text{exi}} = 369\text{ nm}$) displayed yellowish green light emission in the solution state (Table 4, entry 3). Further, CIE colour coordinates have been calculated for the compounds (**4k**–**4p**) which were synthesized from 5-bromoisaatin (**1b**), thiosemicarbazide (**2**) and various α -bromoketones (**3a**, **3b**, **3d**, **3g**, **3i** and **3j**). The study revealed that the compounds **4k** (Ph; $\lambda_{\text{exi}} = 348\text{ nm}$), **4l** (*p*-MePh; $\lambda_{\text{exi}} = 370\text{ nm}$) and **4m** (*p*-FPh;

$\lambda_{\text{exi}} = 370\text{ nm}$) exhibited warm white light emission (Table 4, entries 11–13) whereas **4n** (*m*-BrPh) displayed greenish yellow light emission at $\lambda_{\text{exi}} = 503\text{ nm}$ (Table 4, entry 14), **4o** (β -naphthyl) emitted orange light emission at $\lambda_{\text{exi}} = 372\text{ nm}$ (Table 4, entry 15) and **4p** (coumarinyl) exhibited yellow green light emission at $\lambda_{\text{exi}} = 370\text{ nm}$ (Table 4, entry 16) in the solid state. On the other hand, the compounds **4k** (Ph; $\lambda_{\text{exi}} = 346\text{ nm}$), **4l** (*p*-MePh; $\lambda_{\text{exi}} = 362\text{ nm}$), **4m** (*p*-FPh; $\lambda_{\text{exi}} = 359\text{ nm}$) and **4n** (*m*-BrPh; $\lambda_{\text{exi}} = 352\text{ nm}$) showed purplish blue light emission in the solution state (Table 4, entries 11–14). The compounds **4o** (β -naphthyl; $\lambda_{\text{exi}} = 397\text{ nm}$) and **4p** (4-coumarinyl; $\lambda_{\text{exi}} = 362\text{ nm}$) exhibited yellowish green light emission in the solution state (Table 4, entries 15 and 16). Next, CIE colour coordinates have been calculated for the compounds (**4q**–**4y**) which were synthesized from 5-fluoroisatin (**1c**), thiosemicarbazide (**2**) and various α -bromoketones (**3a**–**3i**). From this investigation, it was observed that the compounds **4q** (Ph; $\lambda_{\text{exi}} = 370\text{ nm}$), **4s** (*p*-OMePh; $\lambda_{\text{exi}} = 370\text{ nm}$), **4t** (*p*-FPh; $\lambda_{\text{exi}} = 368\text{ nm}$), **4v** (*p*-BrPh; $\lambda_{\text{exi}} = 368\text{ nm}$), **4w** (*m*-BrPh; $\lambda_{\text{exi}} = 338\text{ nm}$), **4x** (*p*-CNPh; $\lambda_{\text{exi}} = 368\text{ nm}$) displayed yellow light emission (Table 4, entries 17, 19, 20, 22, 23 and 24) whereas **4r** (*p*-MePh) showed orange light emission at $\lambda_{\text{exi}} = 368\text{ nm}$ (Table 4, entry 18). Interestingly, the compounds, **4u** (*p*-ClPh; $\lambda_{\text{exi}} = 368\text{ nm}$) and **4y** (β -naphthyl; $\lambda_{\text{exi}} = 370\text{ nm}$) emitted warm white light (Table 4, entries 21 and 25) in the solid state. Whereas in the solution state, the compounds **4q** (Ph; $\lambda_{\text{exi}} = 362\text{ nm}$), **4r** (*p*-MePh; $\lambda_{\text{exi}} = 361\text{ nm}$), **4s** (*p*-OMePh; $\lambda_{\text{exi}} = 362\text{ nm}$), **4t** (*p*-FPh; $\lambda_{\text{exi}} = 354\text{ nm}$), **4u** (*p*-ClPh; $\lambda_{\text{exi}} = 360\text{ nm}$), **4x** (*p*-CNPh; $\lambda_{\text{exi}} = 362\text{ nm}$) and **4y** (β -naphthyl; $\lambda_{\text{exi}} = 362\text{ nm}$) emitted blue light emission (Table 4, entries 17–21, 24 and 25). The compounds **4v** (*p*-BrPh; $\lambda_{\text{exi}} = 360\text{ nm}$) and **4w** (*m*-BrPh; $\lambda_{\text{exi}} = 342\text{ nm}$) were showed purplish blue light emission in the solution state (Table 4, entries 22 and 23). Interestingly, the compounds, **4k**, **4l**, **4m**, **4u** and **4y** exhibited warm white light emission in the solid state and this results were supported by the correlated colour temperature (CCT) analysis.

The CCT values are calculated by using the McCamy empirical formula [ref. 64, eqn (1)] to characterize the colour emission and its temperature.

$$\text{CCT} = -449n^3 + 3525n^2 - 6823n + 5520.33 \quad (1)$$

where $n = (x - x_e)/(y - y_e)$ and the chromaticity epicenter is at $x_e = 0.3320$ and $y_e = 0.1858$.

The CCT values of titled compounds (**4**) were calculated that ranging from 2225 K to 3554 K (Table 4). To our delight, the titled compounds, **4k** (2225 K) (orange warm white light), **4l** (2913 K) (warm white light), **4m** (3554 K) (warm white light), **4u** (3001 K) (warm white light) & **4y** (2232 K) (warm white light) were emitted warm white light. It is worthy to mention that the electrochemical behaviour of the synthesized fluorophores has already been reported as ambipolar and hole-transporting materials (HTMs) for optoelectronic applications.⁵⁷ From the photophysical and electrochemical properties, it could be concluded that the white light emissive compounds **4k**, **4l**, **4m**, **4u** and **4y** can act as both hole-transport and ambipolar materials, hence, the cost and size of WOLED devices can be reduced.



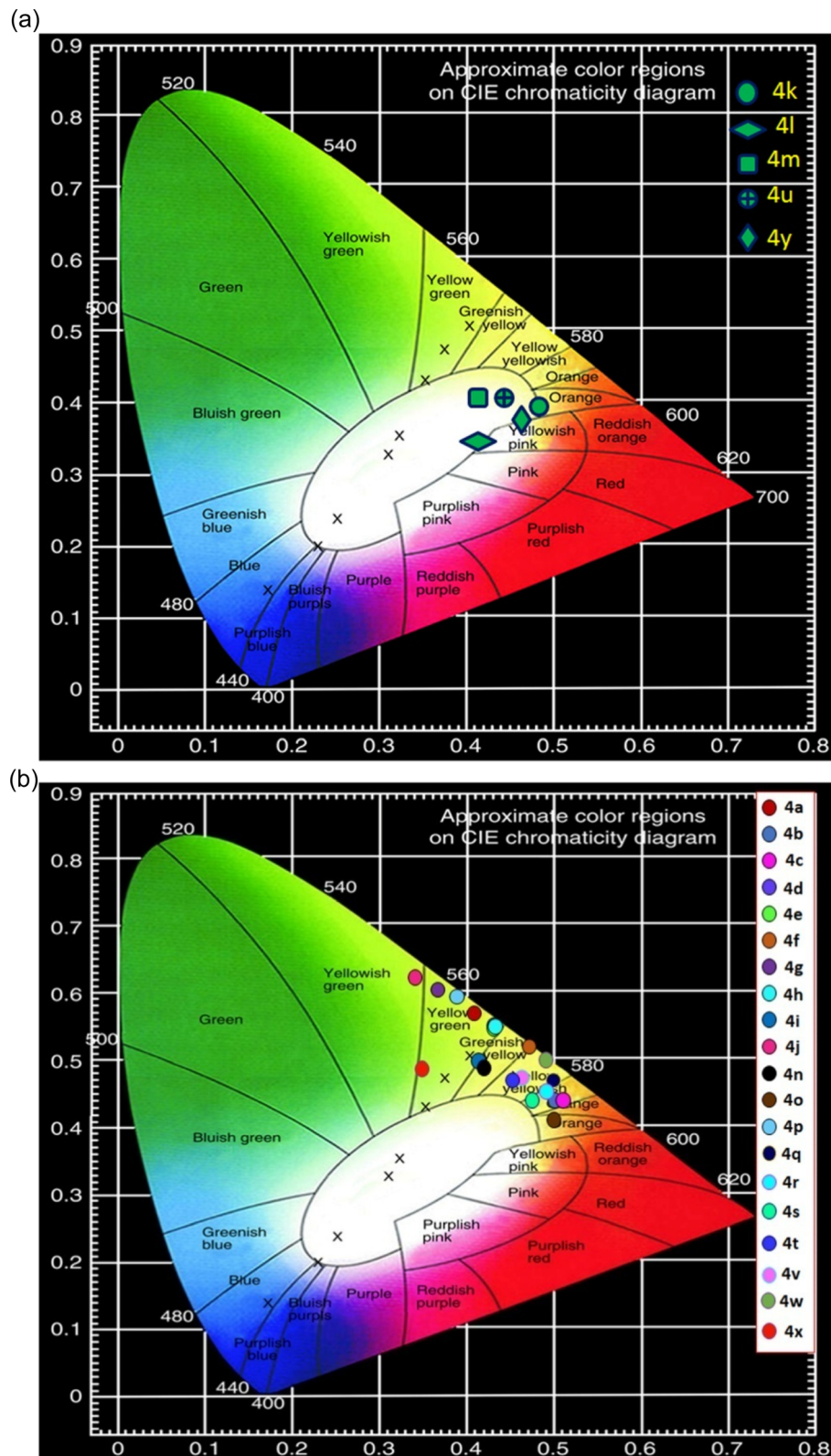


Fig. 4 (a) CIE chromaticity diagram of solid state white light emissive **4k**, **4l**, **4m**, **4u** and **4y**. (b) CIE chromaticity diagram of other thiazolyhydrazoneindolin-2-ones (**4a**–**4j**, **4n**–**4t** and **4v**–**4x**) in the solid state.

The quantum yields (QYs) of white light emissive titled compounds, **4k**, **4l**, **4m**, **4u** and **4y** in the solid state have been determined by using CREE-make YAG:Ce³⁺ as a standard

reference. The QYs of the reference and the abovementioned compounds (**4k**, **4l**, **4m**, **4u** and **4y**) were measured as dispersed powders on quartz slides to simulate their usage in white LED



applications. Identical conditions were maintained to ensure consistency. The QYs (%) of white light emissive compounds, **4k**, **4l**, **4m**, **4u** and **4y** were found to be 0.56, 0.21, 0.32, 0.31 and 0.21, respectively, in the solid state.

Experimental section

General experimental information

All chemicals and solvents were purchased from commercial sources (Sigma-Aldrich, Acros Organics Ltd., Avra, and Merck) and were used as received. α -Bromoketones (**3**) were prepared as per the reported procedure in the literature.⁶⁵ The progress of the reactions was monitored by TLC using 0.25 mm Merck silica gel plates and the spots were visualized under UV light. The ^1H -NMR spectra were recorded on a Bruker NMR spectrometer (400 MHz). Mass spectra were recorded on Shimadzu-LCMS-2010A mass spectrometer. The absorbance spectra were taken using a Shimadzu model UV-3100 UV-visible spectrophotometer. Emission and excitation spectra were recorded on Hitachi fluorescence spectrophotometer (F-2710). Deconvolution analysis of absorption and emission spectral data were carried out by using PeakFit 4.12 version.

Typical experimental procedure for synthesis of thiazolylhydrazoneindolin-2-ones (**4**)

A mixture of isatins (**1**) (5.0 mmol), thiosemicarbazide (**2**) (5.0 mmol), α -bromoketones (**3**) (5.0 mmol), 0.1 N citric acid (5.0 mL) and ethanol (3.0 mL) was stirred at reflux conditions for 40–60 min. The reaction progress was monitored by TLC. Upon completion of the reaction, the mixture was cooled to room temperature and the obtained crude product (**4**) was extracted twice with ethyl acetate (2×5 mL). The resulting organic layer was dried over anhydrous MgSO_4 , volatiles were removed and the obtained product (**4**) was recrystallized from ethanol.

Scale-up procedure for the synthesis of 3-(2-(4-(4-bromophenyl)thiazol-2-yl)hydrazone)indolin-2-one (**4f**)

A mixture of isatin (**1**) (0.0362 mol), thiosemicarbazide (**2**) (0.0362 mol), 2,4'-dibromoacetophenone (**3f**) (0.0362 mol), 0.1 N citric acid (30.0 mL) and ethanol (20.0 mL) was stirred at reflux conditions for 60 min. The reaction progress was monitored by TLC. Upon completion of the reaction, the mixture was cooled to room temperature and the obtained crude product (**4**) was extracted twice with ethyl acetate (2×25 mL). The resulting organic layer was dried over anhydrous MgSO_4 , volatiles were removed and the obtained product (**4f**) was recrystallized from ethanol.

Procedure adapted for quantum yield measurements

The standard reference, cerium-doped yttrium aluminum garnet (YAG:Ce³⁺) and the white light emissive samples (**4k**, **4l**, **4m**, **4u** and **4y**) were finely ground and uniformly coated on quartz slides. The layer thickness was optimized to ensure low optical density ($A < 0.1$) at the excitation wavelength. An excitation wavelength (λ_{exi}) of 460 nm was chosen which was corresponding to the blue LED emission commonly used in white

LED fabrication. The emission spectra of the reference and the samples were recorded under identical conditions using the integrating sphere. The integration time, slit widths, and detector gain were kept constant. The absorbance spectra at $\lambda_{\text{exi}} = 450$ nm was measured for both the reference and the samples (**4k**, **4l**, **4m**, **4u** and **4y**). The fraction of light absorbed ($F_{\text{abs,ref}}$ & $F_{\text{abs,samples}}$) and integrated emission intensities (I_{ref} and I_{samples}) obtained from the area under the respective emission spectrum of both reference and the samples were calculated to obtain QYs (Φ_{samples}) using the following formula:

$$\Phi_{\text{samples}} = \Phi_{\text{ref}} \frac{I_{\text{samples}}}{I_{\text{ref}}} \frac{F_{\text{abs,ref}}}{F_{\text{abs,samples}}}$$

where, $\Phi_{\text{ref}} = 0.76$ (QY of the YAG:Ce³⁺ reference).

I_{samples} and I_{ref} : integrated emission intensities of the samples (**4k**, **4l**, **4m**, **4u** and **4y**) and reference, respectively.

$F_{\text{abs,samples}}$ and $F_{\text{abs,ref}}$: fractions of light absorbed by the samples (**4k**, **4l**, **4m**, **4u** and **4y**) and reference, respectively.

Since the measurements were performed in the solid state configuration, the refractive index (η) was assumed to be approximately equal for both the samples, simplifying the calculation by eliminating the refractive index correction term.

Conclusion

Biodegradable citric acid catalyzed 3-component reaction strategy has proved to be a promising synthetic route to develop multi-colour emissive isatin-thiazole based fluorophores (**4**) from readily available isatins (**1**), thiosemicarbazide (**2**) and α -bromoketones (**3**). This reaction proceeds *via* condensation (C=N) and subsequent thiazole formation (C-S & C-N) in a single step operation. This MCR strategy is highlighted by step economy, cleaner reaction profile, simple to perform, broad substrate scope, use of non-toxic solvents/catalysts, good functional group tolerance, gram scale feasibility, column-free purification, high product yields (91–98%) in a shorter reaction times *etc*. Gratifyingly, the synthesized isatin-thiazole based luminophores (**4**) displayed substituent-dependent tunable optical properties in both solid and solution states like mega Stoke shifts and multi-colour emissions. Thus, the developed multi-colour emissive isatin-thiazole based molecular hybrids could be employed as promising candidates for the fabrication of organic opto-electronic devices. Further, it is worthy to conclude that the compounds, **4k**, **4l**, **4m**, **4u** and **4y** emitted white light in the solid state with mega Stokes shifts.

Data availability

The NMR and mass spectral data supporting this article have been included as part of the ESI.†

Conflicts of interest

The authors declare that they have no known competing financial interests or personal relationships that could have appeared to influence the work reported in this paper.



Acknowledgements

N. C. G. Reddy acknowledges Science and Engineering Research Board (SERB), Department of Science and Technology (DST), New Delhi, India (Project No. SUR/2022/000967) for financial assistance. Shaik Sultana acknowledges the DST, New Delhi for awarding INSPIRE fellowship (IF190786) to do the PhD work.

References

- 1 S.-J. Zou, Y. Shen, F.-M. Xie, J.-D. Chen, Y.-Q. Li and J.-X. Tang, Recent advances in organic light-emitting diodes: toward smart lighting and displays, *Mater. Chem. Front.*, 2020, **4**, 788–820, DOI: [10.1039/c9qm00716d](https://doi.org/10.1039/c9qm00716d).
- 2 R. Kabe, N. Notsuka, K. Yoshida and C. Adachi, After glow organic light-emitting diode, *Adv. Mater.*, 2016, **28**, 655–660, DOI: [10.1002/adma.201504321](https://doi.org/10.1002/adma.201504321).
- 3 L.-S. Cui, A. J. Gillett, S.-F. Zhang, H. Ye, Y. Liu, X.-K. Chen, Z.-S. Lin, E. W. Evans, W. K. Myers, T. K. Ronson, H. Nakamoto, S. Reineke, J.-L. Bredas, C. Adachi and R. H. Friend, Fast spin-flip enables efficient and stable organic electroluminescence from charge-transfer states, *Nat. Photonics*, 2020, **14**, 636–642, DOI: [10.1038/s41566-020-0668-z](https://doi.org/10.1038/s41566-020-0668-z).
- 4 Y. H. Kim, Y. Zhai, H. Lu, X. Pan, C. Xiao, E. A. Gaulding, S. P. Harvey, J. J. Berry, Z. V. Vardeny, J. M. Luther and M. C. Beard, Chiral-induced spin selectivity enables a room-temperature spin light-emitting diode, *Science*, 2021, **371**, 1129–1133, DOI: [10.1126/science.abf5291](https://doi.org/10.1126/science.abf5291).
- 5 Z. Chen, W. Li, M. A. Sabuj, Y. Li, W. Zhu, M. Zeng, C. S. Sarap, M. M. Huda, X. Qiao, X. Peng, D. Ma, Y. Ma, N. Rai and F. Huang, Evolution of the electronic structure in open-shell donor-acceptor organic semiconductors, *Nat. Commun.*, 2021, **12**, 5889, DOI: [10.1038/s41467-021-26173-3](https://doi.org/10.1038/s41467-021-26173-3).
- 6 S. Izumi, H. F. Higginbotham, A. Nyga, P. Stachelek, N. Tohnai, P. Silva, P. Data, Y. Takeda and S. Minakata, Thermally activated delayed fluorescent donor-acceptor-donor-acceptor π -conjugated macrocycle for organic light-emitting diodes, *J. Am. Chem. Soc.*, 2020, **142**, 1482–1491, DOI: [10.1021/jacs.9b11578](https://doi.org/10.1021/jacs.9b11578).
- 7 S. O. Jeon, K. H. Lee, J. S. Kim, S.-G. Ihn, Y. S. Chung, J. W. Kim, H. Lee, S. Kim, H. Choi and J. Y. Lee, High-efficiency, long-lifetime deep-blue organic light-emitting diodes, *Nat. Photonics*, 2021, **15**, 208–215, DOI: [10.1038/s41566-021-00763-5](https://doi.org/10.1038/s41566-021-00763-5).
- 8 S.-J. Zou, Y. Shen, F.-M. Xie, J.-D. Chen, Y.-Q. Li and J.-X. Tang, Recent advances in organic light-emitting diodes: toward smart lighting and displays, *Mater. Chem. Front.*, 2020, **4**, 788, DOI: [10.1039/C9QM00716D](https://doi.org/10.1039/C9QM00716D).
- 9 G. Hong, X. Gan, C. Leonhardt, Z. Zhang, J. Seibert, J. M. Busch and S. Bräse, A Brief History of OLEDs-Emitter Development and Industry Milestones, *Adv. Mater.*, 2021, **33**, 2005630, DOI: [10.1002/adma.202005630](https://doi.org/10.1002/adma.202005630).
- 10 M. Kumar Bera, C. Chakraborty and S. Malik, Solid state emissive organic fluorophores with remarkable broad color tunability based on aryl substituted buta-1,3-diene as the central core, *J. Mater. Chem. C*, 2017, **5**, 6872–6879, DOI: [10.1039/C6TC04906K](https://doi.org/10.1039/C6TC04906K).
- 11 G. Shi, H. Ge, L. Zhang, Y. Li, R. Cui, L. J. Wayment, Y. Ge and W. Zhang, Organic fluorophores with high photostability and strong emission in both solution and solid state, *J. Lumin.*, 2023, **253**, 119447, DOI: [10.1016/j.jlumin.2022.119447](https://doi.org/10.1016/j.jlumin.2022.119447).
- 12 S. Sasaki, G. P. C. Drummen and G. Konishi, Recent advances in twisted intramolecular charge transfer (TICT) fluorescence and related phenomena in materials chemistry, *J. Mater. Chem. C*, 2016, **4**, 2731–2743, DOI: [10.1039/C5TC03933A](https://doi.org/10.1039/C5TC03933A).
- 13 J. Kido, M. Kimura and K. Nagai, Multilayer White Light-Emitting Organic Electroluminescent Device, *Science*, 1995, **267**, 1332–1334, DOI: [10.1126/science.267.5202.1332](https://doi.org/10.1126/science.267.5202.1332).
- 14 S. Reineke, F. Lindner, G. Schwartz, N. Seidler, K. Walzer, B. Lüssem and K. Leo, White Organic Light-Emitting Diodes with Fluorescent Tube Efficiency, *Nature*, 2009, **459**, 234–238, DOI: [10.1038/nature08003](https://doi.org/10.1038/nature08003).
- 15 G. M. Farinola and R. Ragni, Electroluminescent Materials for White Organic Light Emitting Diodes, *Chem. Soc. Rev.*, 2011, **40**, 3467–3482, DOI: [10.1039/C0CS00204F](https://doi.org/10.1039/C0CS00204F).
- 16 L. Ying, C.-L. Ho, H. B. Wu, Y. Cao and W.-Y. Wong, White Polymer Light-Emitting Devices for Solid-State Lighting: Materials, Devices, and Recent Progress, *Adv. Mater.*, 2014, **26**, 2459–2473, DOI: [10.1002/adma.201304784](https://doi.org/10.1002/adma.201304784).
- 17 Q. Wang and D. G. Ma, Management of charges and excitons for high-performance white organic light-emitting diodes, *Chem. Soc. Rev.*, 2010, **39**, 2387–2398, DOI: [10.1039/B909057F](https://doi.org/10.1039/B909057F).
- 18 J. Meyer, S. Hamwi, M. Kröger, W. Kowalsky, T. Riedl and A. Kahn, Transition Metal Oxides for Organic Electronics: Energetics, Device Physics and Applications, *Adv. Mater.*, 2012, **24**, 5408–5427, DOI: [10.1002/adma.201201630](https://doi.org/10.1002/adma.201201630).
- 19 X. L. Yang, G. J. Zhou and W.-Y. Wong, Recent design tactics for high performance white polymer light-emitting diodes, *J. Mater. Chem. C*, 2014, **2**, 1760–1778, DOI: [10.1039/C3TC31953A](https://doi.org/10.1039/C3TC31953A).
- 20 S. Ito, Recent advances in mechanochromic luminescence of organic crystalline compounds, *Chem. Lett.*, 2021, **50**, 649–660, DOI: [10.1246/cl.2000874](https://doi.org/10.1246/cl.2000874) and references therein.
- 21 Y. Tsuchiya, K. Yamaguchi, Y. Miwa, S. Kutsumizu, M. Minoura and T. Murai, *N,N*-Diarylthiazol-5-amines: structure-specific mechanofluorochromism and white light emission in the solid state, *Bull. Chem. Soc. Jpn.*, 2020, **93**, 927–935, DOI: [10.1246/bcsj.202000083](https://doi.org/10.1246/bcsj.202000083).
- 22 S. Sultana, G. Kumar, L. S. Sarma, V. Venkatramu and N. C. Gangi Reddy, Nitrogen-doped TiO_2 nanotubes-catalyzed synthesis of small D- π -A-type Knoevenagel adducts and β -enaminones, *Eur. J. Org. Chem.*, 2023, **26**, e202300032, DOI: [10.1002/ejoc.202300032](https://doi.org/10.1002/ejoc.202300032).
- 23 G. Kumar, S. Sultana, P. M. Khaja Mohinuddin, G. Trivikram Reddy, D. V. C. Subramanyam, L. S. Sarma, D. Haranath, V. Venkatramu and N. C. Gangi Reddy, Solid state thiazole-based fluorophores: promising materials for white organic light emitting devices, *Dyes Pigm.*, 2021, **187**, 109077, DOI: [10.1016/j.dyepig.2020.109077](https://doi.org/10.1016/j.dyepig.2020.109077).



24 M. Y. Wong and E. Zysman-Colman, Purely organic thermally activated delayed fluorescence materials for organic light-emitting diodes, *Adv. Mater.*, 2017, **29**, 1605444, DOI: [10.1002/adma.201605444m](https://doi.org/10.1002/adma.201605444m).

25 K. Takimiya, I. Osaka, T. Mori and M. Nakano, Organic semiconductors based on [1]benzothieno[3,2-b][1]benzothiophene substructure, *Acc. Chem. Res.*, 2014, **47**, 1493–1502, DOI: [10.1021/ar400282g](https://doi.org/10.1021/ar400282g).

26 I. F. Perepichka, *Handbook of Thiophene-Based Materials*, John Wiley & Sons, Chichester, 2009, DOI: [10.1002/9780470745533.ch19](https://doi.org/10.1002/9780470745533.ch19).

27 S. C. Rasmussen, S. J. Evenson and C. B. McCausland, Fluorescent thiophene-based materials and their outlook for emissive applications, *Chem. Commun.*, 2015, **51**, 4528–4543, DOI: [10.1039/c4cc09206f](https://doi.org/10.1039/c4cc09206f).

28 S. Kato, T. Matsumoto, T. Ishi-i, T. Thiemann, M. Shigeiwa, H. Gorohmaru, S. Maeda, Y. Yamashita and S. Mataka, Strongly red-fluorescent novel donor- π -bridge-acceptor- π -bridge-donor (D- π -A- π -D) type 2,1,3-benzothiadiazoles with enhanced two-photon absorption cross-sections, *Chem. Commun.*, 2004, 2342–2343, DOI: [10.1039/b410016f](https://doi.org/10.1039/b410016f).

29 A. Borissov, Y. K. Maurya, L. Moshniaha, W.-S. Wong, M. Źyla-Karwowska and M. Stępień, Recent advances in heterocyclic nanographenes and other polycyclic heteroaromatic compounds, *Chem. Rev.*, 2022, **122**, 565–788, DOI: [10.1021/acs.chemrev.1c00449](https://doi.org/10.1021/acs.chemrev.1c00449).

30 K. Stippich, D. Weiss, A. Guether, H. Gorls and R. J. Beckert, Novel luminescence dyes and ligands based on 4-hydroxythiazole, *J. Sulfur Chem.*, 2009, **30**, 109–118, DOI: [10.1080/17415990802613369](https://doi.org/10.1080/17415990802613369).

31 J. Liebscher, *Houben-Weyl's Methoden der Organischen Chemie*, Georg Thieme Verlag, Stuttgart, 1994.

32 S. K. Manjal, R. Kaur, R. Bhatia, K. Kumar, V. Singh, R. Shankar, R. Kaur and R. K. Rawal, Synthetic and medicinal perspective of thiazolidinones: a review, *Bioorg. Chem.*, 2017, **75**, 406–423, DOI: [10.1016/j.bioorg.2017.10.014](https://doi.org/10.1016/j.bioorg.2017.10.014).

33 R. Mishra, P. K. Sharma, P. K. Verma, I. Tomer, G. Mathur and P. K. Dhakad, Biological potential of thiazole derivatives of synthetic origin, *J. Heterocycl. Chem.*, 2017, **54**, 2103–2115, DOI: [10.1002/jhet.2827](https://doi.org/10.1002/jhet.2827).

34 X. Guo, B. Zhao, Z. Fan, D. Yang, N. Zhang, Q. Wu, B. Yu, S. Zhou, T. A. Kalinina and N. P. Belskaya, Discovery of novel thiazole carboxamides as antifungal succinate dehydrogenase inhibitors, *J. Agric. Food Chem.*, 2019, **67**, 1647–1655, DOI: [10.1021/acs.jafc.8b06935](https://doi.org/10.1021/acs.jafc.8b06935).

35 L. Chen, Y.-J. Zhu, Z.-J. Fan, X.-F. Guo, Z.-M. Zhang, J.-H. Xu, Y.-Q. Song, M. Y. Yurievich, N. P. Belskaya and V. A. Bakulev, Synthesis of 1,2,3-thiadiazole and thiazole-based strobilurins as potent fungicide candidates, *J. Agric. Food Chem.*, 2017, **65**, 745–751, DOI: [10.1021/acs.jafc.6b05128](https://doi.org/10.1021/acs.jafc.6b05128).

36 K. Izawa and T. Onishi, Industrial syntheses of the central core molecules of HIV protease inhibitors, *Chem. Rev.*, 2006, **106**, 2811, DOI: [10.1021/cr050997u](https://doi.org/10.1021/cr050997u).

37 R. M. Lopes and G. Schwartzmann, Natural products in anticancer therapy, *Curr. Opin. Pharmacol.*, 2001, **1**, 364, DOI: [10.1016/S1471-4892\(01\)00063-7](https://doi.org/10.1016/S1471-4892(01)00063-7).

38 N. H. Jayarama, K. Pillwein, R. N. Craig, R. Hoffman and G. Weber, Selective sensitivity to tiazofurin of human leukemic cells, *Biochem. Pharmacol.*, 1986, **35**, 2029, DOI: [10.1016/0006-2952\(86\)90737-9](https://doi.org/10.1016/0006-2952(86)90737-9).

39 D. Lednicer, L. A. Mitscher and G. I. George, *Organic Chemistry of Drug Synthesis*, Wiley, New York, USA, 1990, vol. 4, p. 95.

40 A. Medvedev, O. Buneeva, O. Gnedenko, V. Fedchenko, M. Medvedeva, Y. Ivanov, V. Glover and M. Sandler, Isatin interaction with glyceraldehyde-3-phosphate dehydrogenase, a putative target of neuroprotective drugs: partial agonism with deprenyl, *J. Neural Transm., Suppl.*, 2006, **71**, 97–103, DOI: [10.1007/978-3-211-33328-0_11](https://doi.org/10.1007/978-3-211-33328-0_11).

41 A. Andreani, S. Burnelli, M. Granaiola, A. Leoni, A. Locatelli, R. Morigi, M. Rambaldi, L. Varoli, M. A. Cremonini, G. Placucci and R. Cervellati, New isatin derivatives with antioxidant activity, *Eur. J. Med. Chem.*, 2010, **45**, 1374–1378, DOI: [10.1016/j.ejmech.2009.12.035](https://doi.org/10.1016/j.ejmech.2009.12.035).

42 P. K. Sharma, S. Balwani, D. Mathur, S. Malhotra, B. K. Singh, A. K. Prasad, C. Len, E. V. Eycken, B. Ghosh, N. G. Richards and V. S. Parmar, Synthesis and anti-inflammatory activity evaluation of novel triazolyl-isatin hybrids, *J. Enzyme Inhib. Med. Chem.*, 2016, **31**, 1520, DOI: [10.3109/14756366.2016.1151015](https://doi.org/10.3109/14756366.2016.1151015).

43 C. R. Prakash, S. Raja and G. Saravanan, Design and synthesis of 4-(1-(4-chlorobenzyl)-2,3-dioxoindolin-5-yl)-1-(4-substituted/unsubstituted benzylidene)semicarbazide: novel agents with analgesic, anti-inflammatory and ulcerogenic properties, *Chin. Chem. Lett.*, 2012, **23**, 541, DOI: [10.1016/j.cclet.2012.03.014](https://doi.org/10.1016/j.cclet.2012.03.014).

44 Y. Gao, S. Ma, X. Ya, J. Gao, S. Han, T. Li, Y. Gao and B. Zhao, A novel isatin-based fluorescent chemosensor: synthesis and recognition behaviour towards Fe(III) and PPI in aqueous solution and living cells, *Tetrahedron Lett.*, 2019, **61**, 151452, DOI: [10.1016/j.tetlet.2019.151452](https://doi.org/10.1016/j.tetlet.2019.151452).

45 A. Kundu, S. Pathak and A. Pramanik, Synthesis and Fluorescence Properties of Isatin-Based Spiro Compounds: Switch off Chemo Sensing of Copper(II) Ions, *Asian J. Org. Chem.*, 2013, **2**, 869–876, DOI: [10.1002/ajoc.201300153](https://doi.org/10.1002/ajoc.201300153).

46 D. M. D'Souza, C. Muschelknautz, F. Rominger and T. J. Müller, Unusual Solid-State Luminescent Push-Pull Indolones: A General One-Pot Three-component Approach, *Org. Lett.*, 2010, **12**(15), 3364–3367, DOI: [10.1021/ol101165m](https://doi.org/10.1021/ol101165m).

47 Q. F. Xiang, F. Wang, X. D. Su, Y. J. Liang, L. S. Zheng and Y. J. Mi, Effect of BIBF 1120 on reversal of ABCB1-mediated multidrug resistance, *Cell. Oncol.*, 2011, **34**, 33, DOI: [10.1007/s13402-010-0003-7](https://doi.org/10.1007/s13402-010-0003-7).

48 R. Griffith, M. N. Brown, A. McCluskey and L. K. Ashman, Small molecule inhibitors of protein kinases in cancer-how to overcome resistance, *Mini-Rev. Med. Chem.*, 2006, **6**, 1101, DOI: [10.2174/138955706778560184](https://doi.org/10.2174/138955706778560184).

49 B. Pandit, Y. Sun, P. Chen, D. L. Sackett, Z. Hu, W. Rich, C. Li, A. Lewis, K. Schaefer and P.-K. Li, Structure-activity-relationship studies of conformationally restricted analogs of combretastatin A-4 derived from SU5416, *Bioorg. Med. Chem.*, 2006, **14**, 6492, DOI: [10.1016/j.bmc.2006.06.017](https://doi.org/10.1016/j.bmc.2006.06.017).



50 Z. Xie, G. Wang, J. Wang, M. Chen, Y. Peng, L. Li, B. Deng, S. Chen and W. Li, Synthesis, biological evaluation and molecular docking studies of novel isatin-thiazole derivatives as α -glucosidase inhibitors, *Molecules*, 2017, **22**, 659, DOI: [10.3390/molecules22040659](https://doi.org/10.3390/molecules22040659).

51 W. M. Eldehna, R. I. Al-Wabli, M. S. Almutairi, A. B. Keeton, G. A. Piazza, H. A. Abdel Aziz and M. I. Attia, Synthesis and biological evaluation of certain hydrazoneindolin-2-one derivatives as new potent anti-proliferative agents, *J. Enzyme Inhib. Med. Chem.*, 2018, **33**, 867, DOI: [10.1080/14756366.2018.1462802](https://doi.org/10.1080/14756366.2018.1462802).

52 P. V. Navaneethgowda, D. B. Yadav, B. Manjunatha and K. M. M. Pasha, Some novel isatin-thiazole conjugates and their computational and biological studies, *Struct. Chem.*, 2022, **33**, 897–906, DOI: [10.1007/s11224-022-01892-5](https://doi.org/10.1007/s11224-022-01892-5).

53 S. Sultana, S. Rama Mohana Reddy, G. Kumar, V. Venkatramu, K. Raghava Reddy, B. Ekambaram, N. C. Gangi Reddy and T. M. Aminabhavi, SiO_2 -supported HClO_4 catalyzed synthesis of (*Z*)-thiazolylhydrazoneindolin-2-ones and their electrochemical properties, *Chemosphere*, 2022, **309**, 136667, DOI: [10.1016/j.chemosphere.2022.136667](https://doi.org/10.1016/j.chemosphere.2022.136667).

54 J. Tiwari, S. Singh, F. Tufail, D. Jaiswal, J. Singh and G. Micellar, Glycerol micellar catalysis: an efficient multicomponent-tandem green synthetic approach to biologically important 2,4-disubstituted thiazole derivatives, *ChemistrySelect*, 2018, **3**, 11634–11642, DOI: [10.1002/slct.201802511](https://doi.org/10.1002/slct.201802511).

55 A. Tewdros Birhanu and V. Rajeswar Rao, One pot, multi-component synthesis of 3-[(4-aryl-thiazol-2-yl)-hydrazone]-1,3-dihydro-indole-2-one, *Chem. Res. Chin. Univ.*, 2014, **30**, 601–604, DOI: [10.1007/s40242-014-4036-8](https://doi.org/10.1007/s40242-014-4036-8).

56 M. L. Kondratieva, A. V. Pepeleva, N. P. Belskaia, A. V. Koksharov, P. V. Groundwater, K. Robeyns, L. V. Meervelt, W. Dehaen, Z. J. Fan and V. A. Bakulev, A new synthetic method for the 2*H*-[1,2,3]thiadiazolo[5,4-b]indoles, *Tetrahedron*, 2007, **63**, 3042–3048, DOI: [10.1016/j.tet.2007.01.059](https://doi.org/10.1016/j.tet.2007.01.059).

57 H. Ahankar, A. Ramazani, K. Ślepokura, T. Lis and S. W. Joo, Synthesis of pyrrolidinone derivatives from aniline, an aldehyde and diethyl acetylenedicarboxylate in an ethanolic citric acid solution under ultrasound irradiation, *Green Chem.*, 2016, **18**, 3582, DOI: [10.1039/c6gc00157b](https://doi.org/10.1039/c6gc00157b).

58 J.-H. Zhou, X. Chen, D. Yang, C.-Y. Liu and X.-Y. Zhou, A facile and general oxidative hydroxylation of organoboron compounds: citric acid as an efficient catalyst in water to access phenolic and alcoholic motifs, *Molecules*, 2023, **28**, 7915, DOI: [10.3390/molecules28237915](https://doi.org/10.3390/molecules28237915).

59 G. Trivikram Reddy, G. Kumar and N. C. Gangi Reddy, Citric acid catalyzed synthesis of 2,4-disubstituted thiazoles from ketones via C-Br, C-S and C-N bond formations in one-pot: a green approach, *J. Chin. Chem. Soc.*, 2017, **64**, 1408–1416, DOI: [10.1002/jccs.201700200](https://doi.org/10.1002/jccs.201700200).

60 J. P. Glusker, Citrate conformation and chelation: enzymic implications, *Acc. Chem. Res.*, 1980, **13**, 345–352, DOI: [10.1021/ar50154a002](https://doi.org/10.1021/ar50154a002).

61 N. N. M. Y. Chan, A. Idris, Z. H. Z. Abidin, H. A. Tajuddin and Z. Abdullah, White light employing luminescent engineered large (mega) Stokes shift molecules: a review, *RSC Adv.*, 2021, **11**, 13409, DOI: [10.1039/D1RA00129A](https://doi.org/10.1039/D1RA00129A).

62 J. Yang, Z. Xu, L. Yu, B. Wang, R. Hu, J. Tang, J. Lv, H. Xiao, X. Tan, G. Wang, J.-X. Li, Y. Liu, P.-L. Shao and B. Zhang, Organic Fluorophores with Large Stokes Shift for the Visualization of Rapid Protein and Nucleic Acid Assays, *Angew. Chem., Int. Ed.*, 2024, **63**, e202318800, DOI: [10.1002/anie.202318800](https://doi.org/10.1002/anie.202318800).

63 F. W. Billmeyer and M. Saltzman, *Principles of Colour Technology*, John Wiley & Sons, New York, 1988.

64 C. S. McCamy, Correlated colour temperature as an explicit function of chromaticity coordinates, *Color Res. Appl.*, 1992, **17**, 142–144, DOI: [10.1002/col.5080170211](https://doi.org/10.1002/col.5080170211).

65 B. M. Reddy, V. V. R. Kumar, N. C. Gangi Reddy and S. M. Rao, Silica gel catalyzed α -bromination of ketones using *N*-bromosuccinimide: an easy and rapid method, *Chin. Chem. Lett.*, 2014, **25**, 179, DOI: [10.1016/j.cclet.2013.09.014](https://doi.org/10.1016/j.cclet.2013.09.014).

